Plasticity in Protein-Peptide Recognition: Crystal Structures of Two Different Peptides Bound to Concanavalin A

Deepti Jain, Kanwal J. Kaur, and Dinakar M. Salunke

Structural Biology Unit, National Institute of Immunology, Aruna Asaf Ali Marg, New Delhi 110 067, India

ABSTRACT The structures of concanavalin A (ConA) in complex with two carbohydrate-mimicking peptides, 10-mer (MYWYPYASGS) and 15-mer (RVWYPYGSYLTASGS) have been determined at 2.75 Å resolution. In both crystal structures four independent peptide molecules bind to each of the crystallographically independent subunits of ConA tetramer. The peptides exhibit small but significant variability in conformations and interactions while binding to ConA. The crystal structure of another similar peptide, 12-mer (DVFYPYPYASGS), in complex with ConA has been determined (Jain, D., K. J. Kaur, B. Sundaravadivel, and D. M. Salunke. 2000. Structural and functional consequences of peptide-carbohydrate mimicry. *J. Biol. Chem.* 275:16098–16102). Comparison of the three complexes shows that the peptides bind to ConA at a common binding site, using different contacting residues and interactions depending on their sequence and the local environment at the binding site. The binding is also optimized by corresponding plasticity of the peptide binding site on ConA. The diversity in conformation and interactions observed here are in agreement with the structural leeway concerning plasticity of specific molecular recognition in biological processes. The adaptability of peptide-ConA interactions may also be correlated with the carbohydrate-mimicking property of these peptides.

INTRODUCTION

Concanavalin A (ConA) has been extensively exploited as a model for understanding protein-carbohydrate recognition (Naismith et al., 1994, 1996; Loris et al., 1996; Moothoo et al., 1999). It can also be useful for analyzing the plasticity of protein-peptide interactions, as it also binds to a variety of different peptides of significantly diverse sequences and lengths with comparable affinities. Several different peptides containing Tyr-Pro-Tyr as the consensus sequence motif were identified as ConA ligands based on the screening of a large and diverse peptide library expressed on the surface of filamentous phage (Oldenberg et al., 1992; Scott et al., 1992). The peptides were shown to bind to ConA with affinities comparable to that of methyl α-D-mannopyranoside, a well-characterized carbohydrate ligand of ConA. It was also shown that binding of the 12-mer peptide to ConA could be competitively inhibited by methyl α-D-mannopyranoside in a dose-dependent manner and that the polyclonal antibodies against peptide cross-react with sugar, and vice versa (Kaur et al., 1997), suggesting possible topological equivalence between the two ligands. Furthermore, the crystal structure of 12-mer in complex with ConA revealed that the peptide binding sites were independent of the methyl α-D-mannopyranoside binding site, although the functional mimicry was observed between the two (Jain et al., 2000b; Kaur et al., 2001). However, the structural relationship between 12-mer peptide and carbohydrate moiety in terms of surface topology and their interactions with ConA was evident by independent comparison of the two ligands (Jain et al., 2000a).

Two other peptides, 15-mer and 10-mer, have been characterized to bind to ConA with affinities comparable to those of the 12-mer and methyl α-D-mannopyranoside; 15-mer peptide was identified by screening the phage display library (Oldenberg et al., 1992), and 10-mer peptide was a result of subsequent rational design (Kaur et al., 1997). Here, we report the crystal structures of 15-mer and 10-mer as crystalline complexes of ConA and delineate the residues dictating specificity of ConA-peptide interactions in each case. Analysis of the structures and interactions of the four crystallographically independent peptide molecules in each of the two complexes, and comparison of the binding modes for these and the earlier-determined 12-mer peptide, reveal possible structural confines of plasticity associated with protein-peptide recognition.

MATERIALS AND METHODS

Peptide synthesis and purification

The peptides were synthesized, on an automated peptide synthesizer model 431A (Applied Biosystems, Foster City, CA), as described earlier (Kaur et al., 1997) using solid phase 9-fluorenylmethyloxycarbonyl (Fmoc) chemistry. The crude peptides were purified on a Waters Deltapak reverse-phase C18–100 Å (19 × 300 mm, 15 μm, spherical) column on a preparative HPLC (Waters, Tokyo, Japan) using a linear gradient of water and acetonitrile. The absorption was monitored at 214 nm. Characterization was performed by molecular mass determination using a single quadruple mass analyzer (Fisons Instruments, Altrincham, UK).

Crystallization and data collection

Co-crystallization of ConA (Sigma, St. Louis, MO) at a concentration of 0.32 mM and peptides (15-mer and 10-mer) was carried out using a

Received for publication 19 September 2000 and in final form 19 March 2001.

Address reprint requests to Dr. Dinakar M. Salunke, Structural Biology Unit, National Institute of Immunology, Aruna Asaf Ali Marg, New Delhi 110 067, India. Tel.: 91-11-616-7623, ext. 234; Fax: 91-11-616-2125; E-mail: dinakar@nii.res.in.

0006-3495/01/06/2912/10 $2.00

hanging drop method. Crystals of 10-mer complex were obtained using sodium sulfate as the precipitating agent at pH 7.5, and 15-mer was crystallized in ammonium sulfate at pH 9.0; 50 mM Tris buffer was used in both cases and 20-fold molar excess of peptide has been used for crystallization. The crystallization plates were maintained at room temperature. Crystals grew between 10 and 15 days.

The x-ray intensity data for various ConA-peptide complex crystals were collected on an Image Plate detector (Marresearch, Hamburg, Germany) installed on a rotating anode x-ray source (Rigaku, Tokyo, Japan) operated at 40 kV and 70 mA. The cell dimensions were large, and therefore the crystal-to-detector distance was kept at 235 mm, and 0.25° oscillation frames were recorded to spatially resolve the spots. The data sets were collected up to 2.75 Å resolution in each case. For the 15-mer–ConA complex the diffraction data were collected from two different crystals, processed separately using DENZO (Otwinowski, 1993), and subsequently merged using SCALEPACK. The space group symmetry for both the complexes is $C222_1$.

Structure determination and refinement

The dimer of the tetrameric ConA in complex with methyl α-D-mannopyranoside (5CNA) (Naismith et al., 1994) was used as a probe model for rotation/translation function calculations between 8–4 Å resolution. The coordinates for sugar were removed before attempting molecular replacement using AmoRe (Navaza, 1994). The solution was unambiguous and showed presence of two dimers within the asymmetric unit.

The initial model was subjected to rigid body refinement in X-PLOR to refine orientation and position of the starting model in the unit cell. Initially, dimer was treated as a rigid body and subsequently each monomer was treated independently as a rigid body. The individual atoms were then refined by several cycles of conventional positional refinement with overall B-values. Higher resolution data up to 2.75 Å were added in a stepwise fashion. Both conventional R-factor (R_{cryst}) and the free R-value (R_{free}) (Brünger, 1992) were used to monitor the progress of refinement. An independent set of reflections (10% for 10-mer and 5% for 15-mer) was set aside for R_{free} value calculation. CNS (Brünger et al., 1998) was used in the later stages of refinements. Some of the loops of the ConA model were rebuilt in the electron density and were displayed with the help of O (Jones et al., 1991) on O_2 (Silicon Graphics Inc., Mountain View, CA). Noncrystallographic symmetry restraints with a weight of 120 kCal mol^{-1} $Å^{-2}$ were used for ConA throughout the refinement. This was followed by iterative rebuilding of the peptide models on the basis of 2Fo-Fc and Fo-Fc maps. The average occupancies of the residues in the peptides were slightly lower (between 0.7 and 0.8) than the average occupancy of the protein residues, although they were distinctly above the solvent densities. The Fo-Fc and 2Fo-Fc electron density maps were calculated using the CCP4 package (CCP4, 1994). Water molecules were included in the model using an electron density cutoff of 2.5σ in Fo-Fc and 1σ in 2Fo-Fc, and if they were within 3.5 Å from one or more nitrogen or oxygen atoms of the protein or other water molecule.

RESULTS

Overall structures

The structures of ConA–15-mer and ConA–10-mer complexes have been determined and analyzed extensively. The crystals are isomorphous to those of the ConA–12-mer complex (Jain et al., 2000b). Table 1 shows the refinement statistics of the two complexes. The asymmetric unit in both cases contains four monomers arranged as two dimers (AB and CD) of ConA. The four crystallographically independent monomers (A, B, C, D) in the asymmetric unit bind to four peptide molecules (P, Q, R, S), respectively. The subscripts "15" and "10" are used hereafter for distinguishing the two peptides in 15-mer and 10-mer complexes, respectively. Fig. 1 depicts the representative Fo-Fc electron density maps of one of the conformations of the two peptide ligands. The three-dimensional structure of ConA in complex with 15-mer and 10-mer agrees well with the 12-mer bound form in overall features (Jain et al., 2000b).

TABLE 1 Crystal data and refinement statistics of ConA in complex with 15-mer and 10-mer

Ligand	15-mer	10-mer
Cell constants (Å)	$a = 103.11$	$a = 102.96$
	$b = 118.55$	$b = 118.33$
	$c = 254.99$	$c = 253.60$
Space group	$C222_1$	$C222_1$
Maximum Resolution (Å)	2.75	2.75
Completeness (%)	78.2	85.5
No. of independent reflections	31696	33187
Multiplicity	2	2
Average (I)/(Sig$I$)	6.2	12.7
Completeness in last shell (2.75–2.88Å) (%)	27	37
R_{merge} (%)	10.2	6.0
No. of solvent atoms/asymmetric unit	258	307
rms deviation bond length (Å)	0.008	0.007
rms deviation bond angles (degrees)	1.711	1.587
R_{cryst} (%)	19.5	18.8
R_{free} (%)	24.0	22.2
B factors, overall ($Å^2$)	35.79	40.22

The structure of ConA is similar in both complexes, although some local conformational differences in certain loop regions were observed. The root-mean-square (rms) deviations among four ConA subunits within the asymmetric unit for 15-mer and 10-mer complexes lie within 0.47 Å and 0.38 Å, respectively. The structures were unambiguously assigned, with the exception of the region consisting of residues 116–124, which had comparatively weaker electron density. Besides this region, another loop (residues 200–206) shows variations in conformation within the asymmetric unit. This loop is involved in peptide binding. The backbone conformation of this loop in A and B subunits is equivalent to D and C subunits, respectively. The rms deviation for this loop between A and B subunits is 1.64 Å in case of 10-mer and 1.98 Å in case of 15-mer. Apart from the differences in the backbone conformation, there are smaller but noticeable differences in side-chain orientations in the residues of this loop in different subunits.

The molecular packing in the crystals is such that the symmetry environments of P and Q are quasi-equivalent to S and R conformations, respectively. The conformations P and S bind to ConA such that the contacts with symmetry-related molecules are not significant. These correspond to the P1 binding mode as defined earlier for the 12-mer–ConA complex (Jain et al., 2000b). The Q and R conformations are sandwiched between two crystallographically related ConA monomers, and hence exhibit symmetry con-

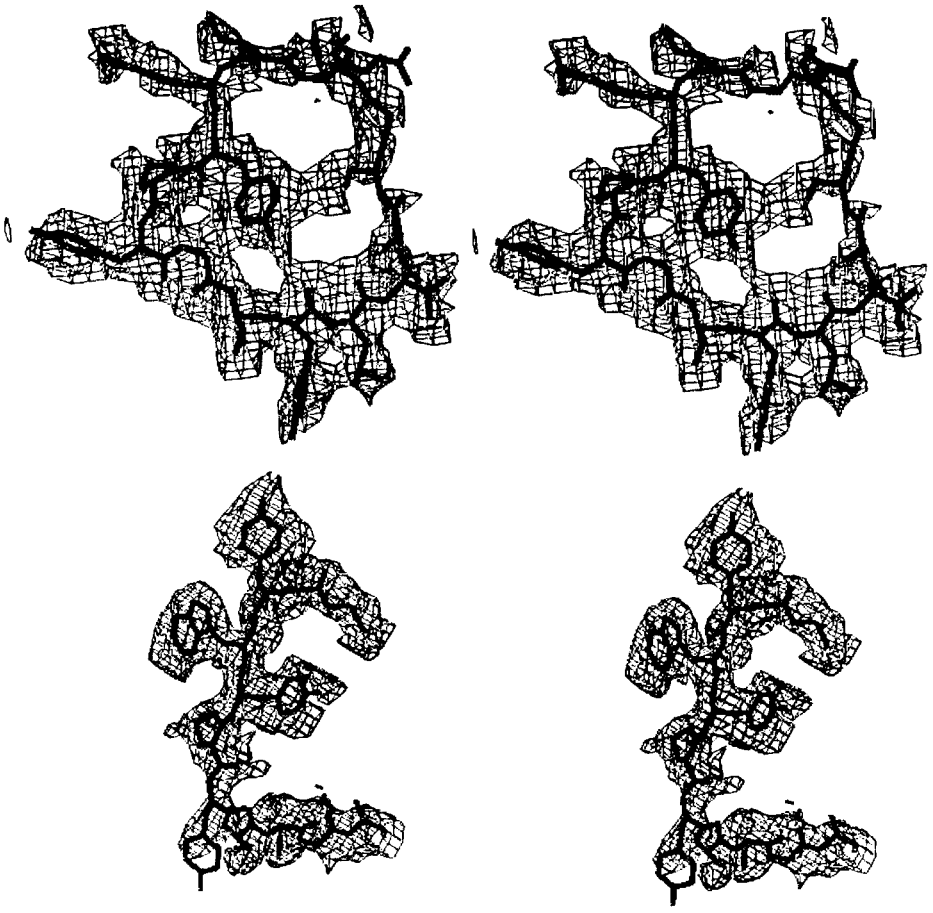

FIGURE 1 Stereoscopic view of the Fo-Fc difference electron density map of the 15-mer and 10-mer bound to ConA.

tacts, which significantly influence the peptide conformations and their interactions. This mode of peptide binding has been referred to as the P2 binding mode in the case of the ConA–12-mer complex. Thus, the peptide binding sites of the subunits A and D, corresponding to P1 binding mode, are solvent-exposed; those of the B and C, corresponding to P2 binding mode, are relatively buried due to crystal packing in all three structures.

Conformation and interactions of the 15-mer

The overall conformation of 15-mer in the asymmetric unit is similar in all four cases (Fig. 2 *A*). The N-terminal residues Arg-1–Tyr-6 of the peptide in all four conformations are extended with a loop formed by residues Gly-7–Leu-10, such that the C-terminus comes in close proximity to the N-terminus. The rms deviation of the Cα superimposition of the peptide conformations independent of ConA is lower (1.69 Å) between the P_{15} and S_{15} as compared to between Q_{15} and R_{15} (3.13 Å). The peptide conformation is stabilized by several intramolecular interactions involving both side chain and main chain atoms. The side chain of N-terminal Arg1:P_{15} forms an intrapeptide salt bridge with a terminal carboxylate group. The backbone structural changes between the four conformations, P_{15}, Q_{15}, R_{15}, and S_{15}, are more prominent for the N-terminal Arg-1, Val-2, and the C-terminal Ala-12–Ser-15 of the peptide, and the rest of the peptide conformation is identical within the two pairs. The superimposition of the four conformations of 15-mer using residues Trp-3–Ala-12 is shown in Fig. 2 *A*.

The P_{15} and S_{15} conformations of 15-mer interact with the respective ConA subunit through Arg-1–Thr-11 at the primary peptide binding site. The Ala-12–Ser-15 stretch does not show any interactions with ConA in both conformations. Although the P_{15} and S_{15} bind at equivalent local environments, there are minor but notable differences in their interactions with ConA, particularly at the N-terminus, as is evident from Table 2. The interactions of Tyr-4–Thr-11 of the peptide are, nonetheless, conserved in both the conformations. The conformational variations were also reflected in the hydrogen-bonding pattern. The residues Ser-8 and Tyr-9 of the peptide form five conserved hydrogen bonds in the two cases. In addition, the Val-2:P_{15} main chain forms a hydrogen bond with the Asn-44:A_{15} side chain. This interaction is absent in S_{15}. Similarly, S_{15} contains two extra hydrogen bonds that are absent in P_{15}. These include the

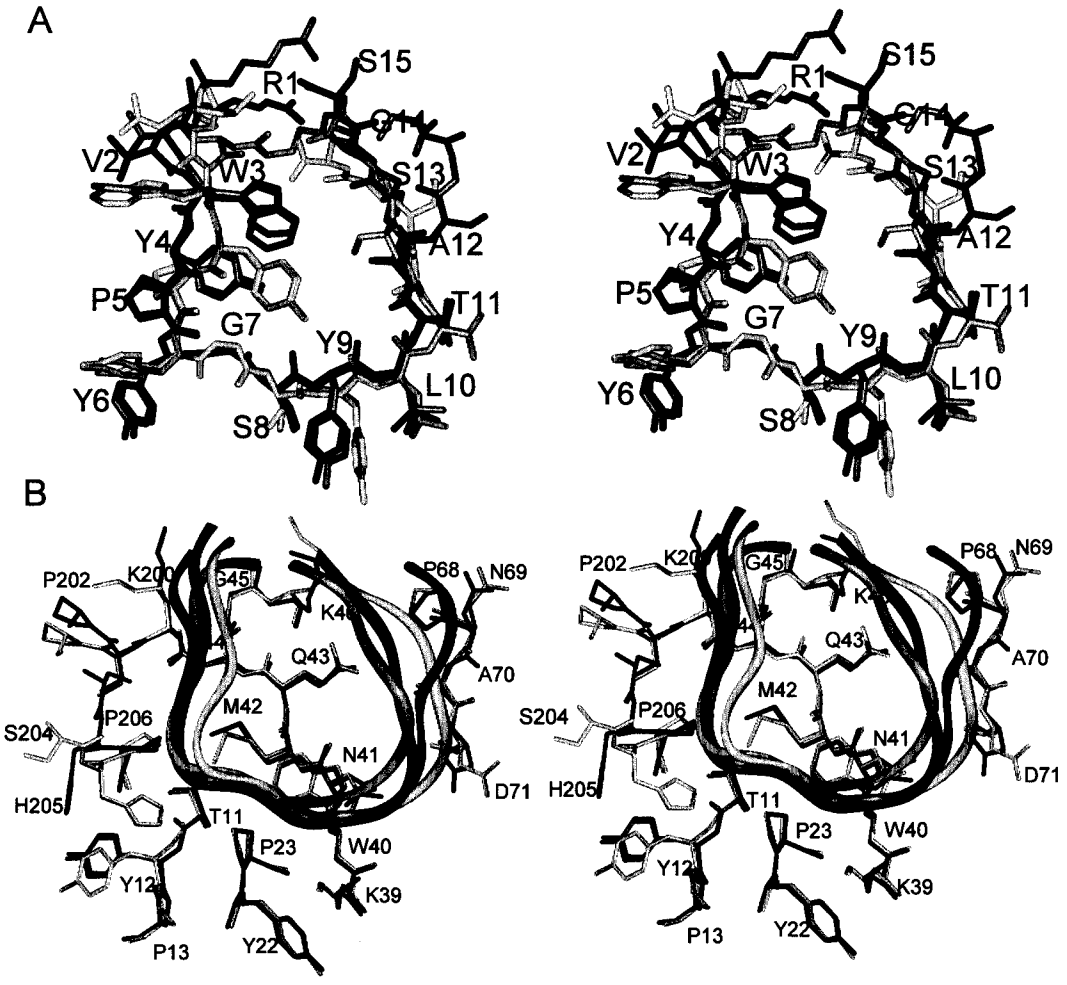

FIGURE 2 Stereoscopic view of the comparison of the independent peptide conformations and interactions of 15-mer within the asymmetric unit. (*A*) The least-squares superimposition of the four peptide conformations P, Q, R, and S using residues Trp-3–Ala-12. (*B*) The four ConA subunits along with their respective bound peptides (drawn as ribbons) are superimposed. Only the interacting residues of ConA within 4 Å distance of the ligand are shown in each case. The P, S, R, and Q are colored in decreasing order of the gray value.

bond between the main chain Trp-3:S_{15} and side chain of Asn-44:D_{15}, and between the side chains of Thr-11:S_{15} and Asp-71:D_{15}. The rms deviation between the two conformations of the peptide on ConA superimposition is 2.5 Å. The buried surface area of P_{15} is higher than S_{15}, although that of ConA in the two cases is comparable (Table 3).

The Q_{15} and R_{15} are sandwiched between two subunits of ConA and show extensive interactions with symmetry equivalents of A_{15} and B_{15} subunits, respectively. The differences in the conformations of Q_{15} and R_{15} are reflected in their interactions as well. The interactions of these conformations with ConA at the primary peptide-binding site involve residues Trp-3–Ser-15 in the case of Q_{15}, and Arg-1–Tyr-9 in the case of R_{15} (Table 2). The contacts of Trp-3, Tyr-4, Ser-8, and Tyr-9 of the peptide are conserved in the two cases. The Gly-7 shows no interactions in either case. The Q_{15} and R_{15} conformations share two conserved hydrogen bonds formed by Ser-8 and Tyr-9 of the peptide. Q_{15} forms five additional hydrogen bonds at the C-terminus and R_{15} forms four hydrogen bonds at the N-terminus and one at the C-terminus. The rms deviation between Q_{15} and R_{15} is 4.97 Å after ConA superimposition. The surface area buried is comparable for Q_{15} and R_{15} (Table 3). The buried surface areas of the peptide conformations in both cases are also close to buried surface areas of the respective ConA subunits, indicating a better complementarity in these subunits as compared to P_{15} and S_{15}. The detailed interactions of each of the four conformations with their respective ConA subunits are depicted in Fig. 2 *B*.

Although the local environments of the peptide binding sites of A (and D) and B (and C) in crystals are different, certain similarities in their interactions with the corresponding peptide molecules could be observed. Trp-3 of 15-mer interacts with Asn-44 in all four subunits. Most of the ConA residues interacting with Tyr-4, Ser-8, and Tyr-9 are conserved. Two hydrogen bonds are conserved between the P1 and P2 binding modes. The rms deviation between P_{15} and Q_{15} and between R_{15} and S_{15} is 4.93 Å and 5.03 Å, respectively, after ConA superimposition.

TABLE 2 van der Waals contacts for the three peptides

15-mer	*P*	*S*	*Q*	*R*	10-mer	*P*	*S*	*Q*	*R*	12-mer	*P*	*S*	*Q*	*R*
R1				G45	M1			G45		D1				
	K46			K46				K46						
											K200	K200		
V2	N44	N44			Y2	N44	N44			V2	N44	N44	N44	N44
				G45									G45	G45
						K200	K200				K200	K200	K200	K200
	S201										S201	S201	S201	S201
	P202													
	S204													
W3		Q43			W3					F3				
	N44	N44	N44	N44		N44	N44	N44	N44				N44	N44
				G45									G45	G45
											K46	K46	K46	K46
			S201	S201				S201	S201					
			P202	P202				P202	P202					
								D203	D203					
Y4	N41	N41			Y4					Y4				
	M42	M42	M42	M42										
	Q43	Q43	Q43	Q43			Q43						Q43	Q43
	N44	N44	N44	N44		N44	N44	N44	N44		N44	N44	N44	N44
									K46		K46	K46	K46	K46
	S204	S204				S204	S204							
P5			N44	N44	P5	N44	N44	N44		P5	N44	N44	N44	N44
											S201	S201		
	S204	S204				S204	S204	S204			S204	S204		
	H205	H205												
	P206	P206		P206		P206	P206							
Y6	T11	T11			Y6					Y6			T11	T11
	Y12	Y12												
	P13	P13												
	P23	P23											P23	P23
	M42	M42											M42	M42
													Q43	Q43
											N44	N44	N44	N44
				S204							S204	S204		
			H205	H205		H205	H205				H205	H205		
	P206	P206									P206	P206	P206	P206
G7	P23	P23								P7	P23	P23		
	W40	W40												
	M42	M42									M42	M42		
											N44	N44		
											P206	P206		
S8										Y8	Y22	Y22		
	P23	P23	P23	P23							P23	P23		
	K39	K39	K39	K39							K39	K39		
	W40	W40	W40	W40							W40	W40		
	N41	N41	N41	N41							N41	N41		
	M42	M42									M42	M42		
Y9	K39	K39	K39	K39										
	N41	N41	N41	N41										
L10	K39	K39												
			N41											
T11	D71	D71	D71											
A12					A7	N41	N41			A9				
						M42	M42							
											Q43	Q43		
											K46	K46		
			N69											
			A70											
			D71											
S13					S8		N41			S10				
						Q43	Q43				Q43	Q43		
			N69											
			A70											
G14			Q43		G9					G11				
			P68											
			N69											
			A70											
S15					S10				N41	S12				
			Q43				Q43				Q43	Q43		
						K46	K46				K46	K46		
									A70					
									D71					

TABLE 3 Buried surface area of four conformations of 15-mer and 10-mer in Å^2

	15-mer		10-mer	
Conformation	Peptide	ConA	Peptide	ConA
P	723.6	565.2	352.2	324.9
Q	533.5	576.2	250.1	255.8
R	554.9	559.7	326.4	306.6
S	685.4	562.9	455.8	407.2

Conformation and interactions of the 10-mer

The 10-mer shows significant conformational variations while binding to the four different subunits of ConA. The N-terminal region Met-1–Tyr-6 of the peptide is extended in all four conformations. This part of the peptide shows less variability in terms of backbone angles. The overall conformations of P_{10} and S_{10} are similar, which is reflected in the low rms deviation (0.79 Å) between the two, calculated independent of ConA. The peptide in these two conformations adopts a folded structure such that the N- and C-terminal residues show intramolecular contacts. However, in the case of Q_{10} and R_{10} the C-terminus is also extended and interacts with the symmetry-related molecule, and hence has different conformations with a higher rms deviation of 3.03 Å, when peptide conformations are superimposed independent of ConA. Superimposition of all four conformations of the 10-mer using residues Tyr-2–Tyr-6 is shown in Fig. 3 *A*.

In the case of P_{10} and S_{10} almost the entire peptide interacts with the corresponding ConA subunit, except Met-1 and Gly-9 (Table 2). Interactions of Tyr-2, Trp-3, and Pro-5–Ala-7 are conserved in the two conformations. P_{10} and S_{10} form five conserved hydrogen bonds with ConA. These are formed by the N-terminal residues of the peptide. In addition, Ser-10:P_{10} forms a hydrogen bond with Lys-46:A_{10}. Similarly, two other hydrogen bonds, between Ala-7:S_{10} and Asn-41:D_{10} and between Ser-8:S_{10} and Asn-41:D_{10}, are absent in the case of P_{10}. The rms deviation on superimposition of the corresponding ConA subunits for the two peptides is 1.99 Å. The buried surface area shows

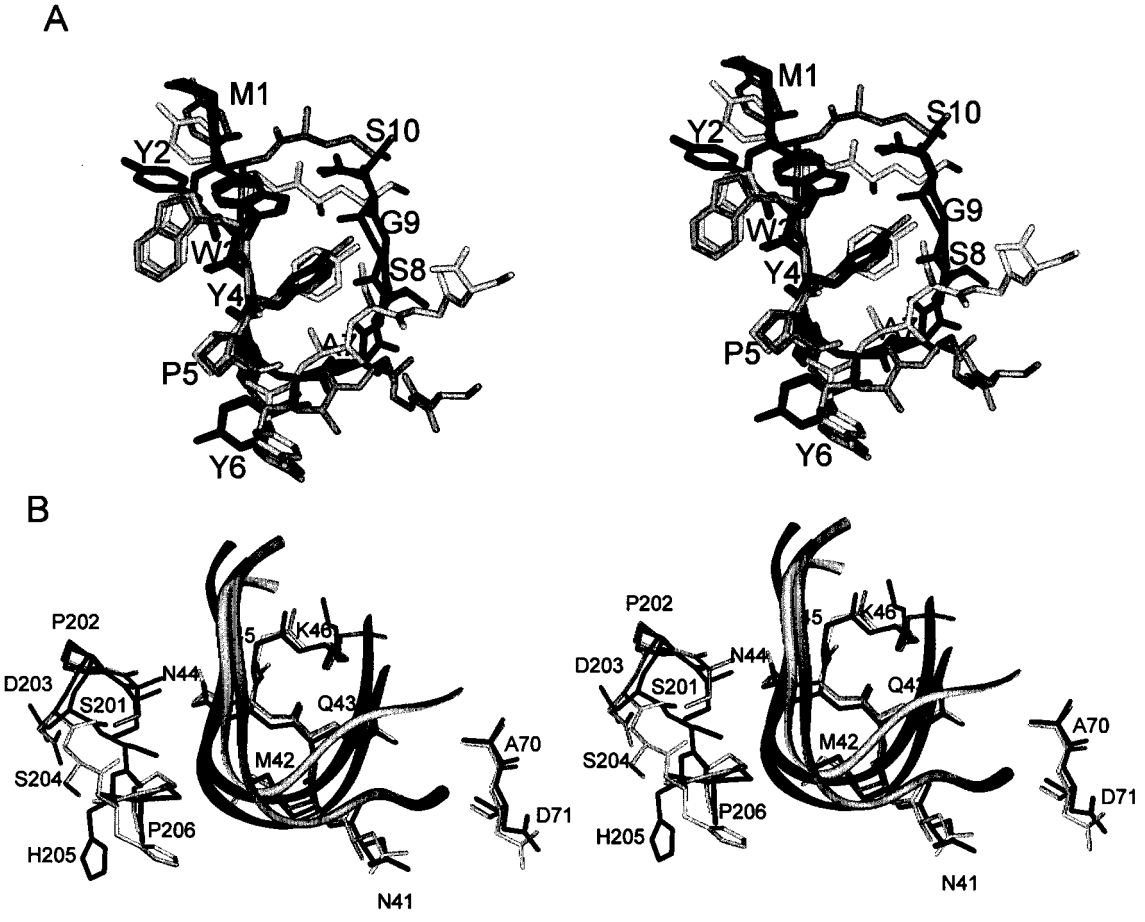

FIGURE 3 Stereoscopic view of the comparison of the independent peptide conformations and interactions of 10-mer within the asymmetric unit. (*A*) The least-squares superimposition of the four peptide conformations P, Q, R, and S using residues Tyr-2–Tyr-6. (*B*) The four ConA subunits along with their respective bound peptides (drawn as ribbons) are superimposed. Only the interacting residues of ConA within 4 Å distance of the ligand are shown in each case. The P, S, R, and Q are colored in decreasing order of the gray value.

significant differences in the two cases, with S_{10} being more than P_{10}, as seen in Table 3.

The Q_{10} and R_{10} conformations are sandwiched between two crystallographically related ConA subunits such that they show extensive van der Waals contacts with the symmetry-related ConA and the peptide. The primary peptide binding site interactions in the two cases include N-terminal residues Met-1:Q_{10}–Pro-5:Q_{10} and Trp-3:R_{10}–Tyr-4:R_{10}. In addition, Ser-10:R_{10} also shows interactions. Conserved interactions were observed only for Trp-3 between the two conformations. The residues Tyr-2 and Tyr-6–Gly-9 show no contacts at all in either case (Table 2). The Trp-3 in Q_{10} and R_{10} form a conserved hydrogen bond with the Asn-44 side chain of the corresponding ConA subunit. In addition, three more hydrogen bonds are formed by Ser-10:Q_{10} that are absent in R_{10}. The rms deviation between R_{10} and S_{10} is 5.53 Å on ConA superimposition. The buried surface area is lower for Q_{10} than R_{10}. Fig. 3 *B* shows the comparison of the interactions of the four conformations of the peptide.

The local packing environments of the peptide binding sites of A (and D) and B (and C) show very few similarities in their interactions with the corresponding peptide molecules. Trp-3 of peptide interacts with Asn-44 in all four subunits. None of the hydrogen bonds appears to be conserved between the two binding modes. The rms deviation between P_{10} and Q_{10} and between R_{10} and S_{10} is 5.05 Å and 5.53 Å, respectively, after ConA superimposition.

Comparison of different ConA binding peptides

Comparison of the conformations and interactions of various peptide ligands—10-mer, 12-mer and 15-mer—bound to ConA exhibits striking differences due to varying lengths and sequences, yet they bind at a common site on ConA. The sequence comparison of the three peptide ligands shows that first six residues can be aligned in each case, although the nature of the first residue varies significantly. Beyond these residues, 15-mer contains five extra residues that form a loop (Table 2). Corresponding residues are absent in 10-mer, and only two residues are present in 12-mer. The sequence Ala-Ser-Gly-Ser, present at the C-terminus, is common to all the three peptides. Structural comparison of the peptides shows substantial conformational overlap at the N-termini, while differences in conformation are obvious toward the C-termini, presumably due to the insertion of varying lengths in 15-mer and 12-mer. The interaction of the P conformation with corresponding ConA in the three peptides is depicted in Fig. 4.

The van der Waals contacts of each of the three peptides, 15-mer, 10-mer, and 12-mer, with ConA are listed in Table 2. Despite the differences, there are certain conserved contacts in the cases of all three peptides. Conserved contacts were observed for the residues of the loop in 15-mer and 12-mer. Gly-7 of the 15-mer and the corresponding Pro-7 of the 12-mer, and Ser-8 of the 15-mer and Tyr-8 of the 12-mer, show significant conserved interactions. Whereas the 15-mer exhibits no contacts, for the last four residues, a few contacts were observed to be conserved between 10-mer and 12-mer. None of the hydrogen bonds is conserved among all three peptides in these two conformations. A comparison of the buried peptide binding sites (Q and R) in the case of the three peptides shows only two conserved contacts: one shown by Trp-3 of the 15-mer and 10-mer and Phe-3 of the 12-mer with Asn-44 of ConA, and the other shown by Tyr-4 of the three peptides and Asn-44 of ConA.

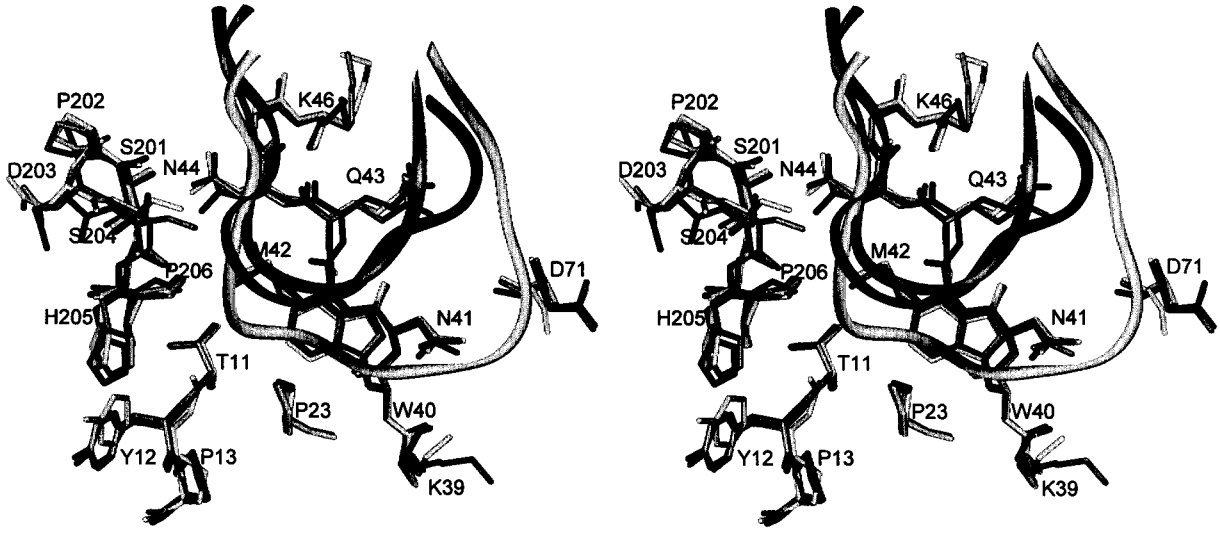

FIGURE 4 Stereoscopic view of the superimposition of the structures and interactions of the peptides bound to the A subunit of ConA in three different crystal structures. Interactions of the three peptides (drawn in ribbons) with the corresponding ConA residues within 4 Å distance of the peptides. The 12-, 10-, and 15-mers are shown in decreasing order of the gray value. The corresponding ConA residues are shown in thin sticks.

However, none of the hydrogen bonds is conserved between the peptides in P2 mode as well.

DISCUSSION

Molecular recognition may exhibit a certain level of degeneracy within the realm of specificity because complementarity of shape and charge can be achieved in more than one way in receptor-ligand recognition (Wilson and Jolliffe, 1999; Morton and Matthews, 1995; Sundberg and Mariuzza, 2000; Sleigh et al., 1999; McEvoy et al., 1998). In several instances a receptor is designed to bind to a number of different ligands: e.g., chaperone proteins (Chen and Sigler, 1999), the MHC molecules (Garcia et al., 1998), polyreactive antibodies (Keitel et al., 1997; Stanfield et al., 1999), and many enzymes (Trautner and Noyer-Weidner, 1992; Bone et al., 1989). When a receptor binds to more than one ligand at a common site, specific recognition could still be achieved either through conservation of a set of crucial interactions (Arevalo et al., 1993; Katz, 1995) or by using altogether different contacting residues of receptor by each ligand (Keitel et al., 1997). Flexibility in the nature of ligand and/or receptor can facilitate such variability in interactions. The most interesting feature of the present study is that the three different peptides bind to ConA at four independent subunits in two different local environments, showing variations in conformations and interactions. In addition, differences were also observed in the peptide conformations bound at the equivalent crystal environments. Thus, the adaptability in structure and interactions was observed at three different levels in ConA-peptide system: a ligand bound in two crystallographically independent but equivalent environments, a ligand bound in two quasi-equivalent environments, and different ligands bound in equivalent environments.

The structure and interactions of the 10-mer and 15-mer bound to the ConA subunits in the pairs of equivalent environments show small but significant differences. The variations were more pronounced at the N-terminal two residues and the C-terminal four residues. Intriguingly, the two peptide molecules bound at the exposed sites (P and S) are conformationally closer to each other than those bound at the buried sites (Q and R). However, the structure and interactions in the case of 12-mers within these sites were identical (Jain et al., 2000b). The buried surface area on peptide-ConA binding, in the equivalent environments, shows significant differences in the case of the 10-mer, and small differences in the case of the 15-mer, consistent with the variations in the corresponding peptide conformations. Albeit, it is anticipated that the ligand would bind to the receptor in identical conformation in the equivalent environments; significant variability was observed in the present model system. The rms deviations in the range of 2 to 5 Å observed in case of the two molecules bound at equivalent sites represent the extent of leeway available in the ConA-peptide recognition without compromising the specificity.

The peptide binding sites in P1 as compared to P2 modes are quasi-equivalent in all three complexes involving 15-, 10-, and 12-mer due to different crystal packing environments. In P2 mode, the C-terminus of the peptide shows extensive interactions with the symmetry-related ConA subunit. Hence, the structures of the peptides and their interactions with ConA in this mode are influenced by symmetry contacts, unlike in the case of P1 mode. The buried surface area in the P1 mode is significantly higher than in the P2 mode for all the three peptides. This is consistent with the fact that the peptides in P2 mode are also stabilized by the interactions with the symmetry-related molecule in the crystals. The rms deviation between P1 and P2 modes is ~5 Å in the case of any of the three peptides. Thus, the peptides exhibit distinct features in terms of structure and interactions in the two quasi-equivalent modes such that the conformational integrity of the ligand is compromised to maintain the specificity of interactions.

The three peptides having fairly different sequences in terms of length and nature of residues that exhibit functional mimicry with carbohydrate ligands (Kaur et al., 1997, 2001) bind to ConA at the same site. They evince significant conformational diversity while overall structural features were shared between them. This diversity may be correlated with their binding affinities to ConA, with K_d values ranging between 0.046 and 0.23 mM (Oldenberg et al., 1992; Kaur et al., 1997). The affinities of these peptides are comparable to that of a well-characterized carbohydrate ligand, methyl α-D-mannopyranose (K_d = 0.089 mM). Thus, the peptides bind to ConA at the same site with comparable affinities involving different sets of residues. A correlation of the extent of variation in the sequences and lengths of the peptides with their conformations and interacting residues in ConA was apparent.

The conserved interacting part of the three ConA binding peptides is the Tyr-Pro-Tyr segment, which accounts for more than half the buried surface area of the peptide in most of the cases. Because conformational variability was minimal for the Tyr-Pro-Tyr segment, it was considered possible that this segment is responsible for the overall specificity of the peptides toward ConA. Possibly, it serves as an anchor for the rest of the peptide to adapt itself for binding to the protein. The maximum rms deviation between them is 2.4 Å, taking all atoms of the motif for superimposition (Table 4). Although the backbone in all the cases superimposes well, there are variations in the side chain conformations that may be induced due to interactions and conformations of the flanking residues. In the context of the conserved Tyr-Pro-Tyr segment in the ConA binding peptides, it was interesting to see the conformational preferences for the Tyr-Pro-Tyr motif in protein structures. Forty-one unique Tyr-Pro-Tyr segments were identified by sequence search in the Brookhaven protein data bank (PDB). Least-square su-

TABLE 4 RMS deviations of backbone atoms between Tyr-Pro-Tyr motifs in four conformations of 15-mer, 12-mer, and 10-mer in Å

	P		*Q*		*R*		*S*	
	15-mer	10-mer	15-mer	10-mer	15-mer	10-mer	15-mer	10-mer
10-mer	0.11		0.12		0.39		0.19	
	(1.34)		(1.44)		(1.83)		(1.43)	
12-mer	0.53	0.42	0.54	0.46	0.51	0.91	0.67	0.47
	(2.16)	(2.40)	(2.30)	(2.23)	(2.39)	(2.05)	(2.23)	(2.40)

The values in parentheses are for all atoms.

perimposition of the backbone atoms led to the identification of two distinct conformational patterns consisting of two-thirds of the Tyr-Pro-Tyr segments showing either type III β-turn (17 structures) or polyproline type II conformation (14 structures) consistent with the similar analysis in the aromatic-proline-aromatic motif (Nagpal et al., 1999). However, the conformation of the Tyr-Pro-Tyr motif observed in the ConA binding peptides does not belong to either of these patterns. Interestingly, the extent of variation observed in the case of these three peptides within the Tyr-Pro-Tyr motif is the same as that found in case of the two structural patterns identified for this motif from PDB.

Adaptability was also evident in the peptide binding site of ConA. The conformations of the loop (200–206) in the equivalent environments within P1 mode or within P2 mode are identical, and show rms deviations within 0.5 Å. However, there are differences in the conformation of the loop between the two quasi-equivalent environments. In fact, the loop conformation is significantly different in P1 mode compared to that in the unliganded ConA (Hardman and Ainsworth, 1972). Earlier studies have shown that this loop is largely disordered in the ConA-trimannose complex (Naismith and Field, 1996). However, the loop is well-ordered in ConA-peptide complexes. Thus, inherent flexibility of this segment indirectly contributes to the plasticity of the peptide binding site, which may be responsible for its ability to bind to peptides of different sequences and lengths. There are several other examples in which conformational variability in the receptor is exploited for binding (Rees et al., 2000; Chen and Sigler 1999).

To conclude, the present study reveals plasticity in peptide-ConA recognition. Assessment of the conformations adopted by various peptide ligands for binding to ConA shows significant degrees of conformational flexibility associated with the peptide binding. It is possible that, in solution, the peptide in complex with a single ConA molecule may be fluctuating among a range of conformations. Thus, the ability of ConA to present a broad spectrum of peptides requires a compromise between conformational space occupied by peptides and specificity of interactions. Conformational variability in the peptides allows a unique binding pattern in each case, yet maintaining the specificity conferred by the Tyr-Pro-Tyr motif. It has been shown earlier that the 15-mer, 12-mer and 10-mer mimic the ConA binding carbohydrates in terms of antibody response (Kaur et al., 1997, 2001). The aromatic nature of the Tyr-Pro-Tyr motif of these peptides corresponds to the aromaticity associated with the carbohydrate moieties (Jain et al., 2000a). This implies that the conformation adopted by the Tyr-Pro-Tyr in these peptides may resemble a region of the complex carbohydrates in some way on cell surfaces that bind to ConA. In fact, the adaptability observed in peptide-ConA recognition is akin to the flexibility seen earlier for ConA-carbohydrate binding (Moothoo et al., 1999; Loris et al., 1996), and it may also be contributing to the molecular mimicry exhibited by them.

This work was supported by the Dept. of Biotechnology (GOI) with funds provided to the National Institute of Immunology. D.J. is the recipient of a fellowship from the CSIR (India).

REFERENCES

Arevalo, J. H., M. J. Taussig, and I. A. Wilson. 1993. Molecular basis of crossreactivity and limits of antibody-antigen complementarity. *Nature.* 365:859–863.

Bone, R., J. L. Silen, and D. Agard. 1989. Structural plasticity broadens the specificity of an engineered protease. *Science.* 339:191–195.

Brünger, A. T. 1992. The free R value: a novel statistical quantity for assessing the accuracy of crystal structures. *Nature.* 355:472–474.

Brünger, A. T., P. D. Adams, G. M. Clore, W. L. DeLano, P. Gros, R. W. Grosse-Kunstleve, J. Jian-Sheng, J. Kuszewski, M. Nilges, N. S. Pannu, R. J. Read, L. M. Rice, T. Simonson, and G. L. Warren. 1998. Crystallography and NMR system: a new software suite for macromolecular structure determination. *Acta Crystallogr.* D54:905–921.

CCP4, SERC Daresbury Laboratory, Warrington, W A4 4AD, England. 1994. The CCP4 suite: programs for protein crystallography. *Acta Crystallogr.* D50:760–763.

Chen, L., and P. B. Sigler. 1999. The crystal structure of a GroEL/peptide complex: Plasticity as a basis for substrate diversity. *Cell.* 99:757–768.

Garcia, K. C., M. Degano, L. R. Pease, M. Huang, P. A. Peterson, L. Teyton, and I. A. Wilson. 1998. Structural basis of plasticity in T cell receptor recognition of a self peptide-MHC antigen. *Science.* 279: 1166–1172.

Hardman, K. D., and C. F. Ainsworth. 1972. Structure of concanavalin A at 2.4 Å resolution. *Biochemistry.* 11:4910–4919.

Jain, D., K. Kaur, M. Goel, and D. M. Salunke. 2000a. Structural basis of functional mimicry between carbohydrate and peptide ligands of ConA. *Biochem. Biophys. Res. Commun.* 272:843–849.

Jain, D., K. J. Kaur, B. Sundaravadivel, and D. M. Salunke. 2000b. Structural and functional consequences of peptide-carbohydrate mimicry. *J. Biol. Chem.* 275:16098–16102.

Jones, T. A., S. Cowan, J. Y. Zou, and M. Kjeldgaard. 1991. Improved methods for building protein models in electron density maps and the location of errors in these models *Acta Crystallogr.* A47:110–119.

Katz, B. A. 1995. Binding of protein targets of peptidic leads discovered by phage display: crystal structures of streptavidin-bound linear and cyclic peptide ligands containing the HPQ sequence. *Biochemistry.* 34: 15421–15429.

Kaur, K. J., D. Jain, M. Goel, and D. M. Salunke. 2001. Immunological implications of structural mimicry between a dodecapeptide and a carbohydrate moiety. *Vaccine*. 19:3124–3130.

Kaur, K. J., S. Khurana, and D. M. Salunke. 1997. Topological analysis of the functional mimicry between a peptide and a carbohydrate moiety. *J. Biol. Chem.* 272:5539–5543.

Keitel, T., A. Kramer, H. Wessner, C. Scholz, J. Schneider-Mergener, and W. Honhe. 1997. Crystallographic analysis of anti-p24 (HIV-1) monoclonal antibody cross-reactivity and polyspecificity. *Cell.* 91:811–820.

Loris, R., D. Maes, F. Poortmans, L. Wyns, and J. Bouckaert. 1996. A structure of the complex between concanavalin A and methyl-3,6-di-O-(α-D-mannopyranosyl)-α-D-mannopyranoside reveals two binding modes. *J. Biol. Chem.* 271:30614–30618.

McEvoy, M., A. C. Hausrath, G. B. Randolph, and S. J. Remington. 1998. Two binding modes reveal flexibility in kinase/response regulator interactions in the bacterial chemotaxis pathway *Proc. Natl. Acad. Sci. U.S.A.* 95:7333–7338.

Moothoo, D. N., B. Canan, R. A. Field, and J. H. Naismith. 1999. Man alpha1→2 Man alpha-OMe-concanavalin A complex reveals a balance of forces involved in carbohydrate recognition. *Glycobiology*. 9:539–545.

Morton, A., and B. W. Matthews. 1995. Specificity of ligand binding in a buried nonpolar cavity of T4 lysozyme: linkage of dynamics and structural plasticity. *Biochemistry.* 34:8576–8588.

Nagpal, S., V. Gupta, K. J. Kaur, and D. M. Salunke. 1999. Structure-function analysis of tritrypticin, an antibacterial peptide of innate immune origin. *J. Biol. Chem.* 274:23296–23304.

Naismith, J. H., C. Emmerich, J. Habash, S. J. Harrop, J. R. Helliwell, W. N. Hunter, J. Raftery, A. J. Kalb (Gilboa), and J. Yariv. 1994. Refined structure of concanavalin A complexed with methyl D-mannopyranoside at 2.0 Å resolution and comparison with the saccharide-free structure *Acta Crystallogr.* D50:847–858.

Naismith, J. H., and R. A. Field. 1996. Structural basis of trimannoside recognition by concanavalin A. *J. Biol. Chem.* 271:972–976.

Navaza, J. 1994. AMoRe: an automated package for molecular replacement. *Acta Crystallogr.* A50:157–163.

Oldenberg, K. R., D. Loganathan, I. J. Goldstein, P. G. Schultz, and M. A. Gallop. 1992. Peptide ligands for a sugar-binding protein isolated from a random peptide library. *Proc. Natl. Acad. Sci. U.S.A.* 89:5393–5397.

Otwinowski, Z. 1993. Oscillation data reduction program. *In* Proceedings of the CCP4 Study Weekend: Data collection and Processing. Sawyer, L., Isaasc, N., and Bailey, S., editors., SERC Daresbury Laboratory, Warrington, UK, 56–62.

Rees, B., G. Webster, M. Delarue, M. Boeglin, and D. Moras. 2000. Aspartyl tRNA-synthetase from *Escherichia coli*: flexibility and adaptability to the substrates. *J. Mol. Biol.* 299:1157–1164.

Scott, J. K., D. Loganathan, R. B. Easly, X. Gong, and I. J. Goldstein. 1992. A family of concanavalin A-binding peptides from hexapeptide epitope library. *Proc. Natl. Acad. Sci. U.S.A.* 89:5398–5402.

Sleigh, S. H., P. R. Seavers, A. J. Wilkinson, J. E. Ladbury, and J. R. Tame. 1999. Crystallographic and calorimetric analysis of peptide binding to OppA protein. *J. Mol. Biol.* 291:393–415.

Stanfield, R. L., E. Cabezas, A. C. Satterthwait, E. A. Stura, A. T. Pfy, and I. A. Wilson. 1999. Dual conformations for the HIV-1 gp120 V3 loop in complexes with different neutralizing Fabs. *Structure.* 7:131–142.

Sundberg, E. J., and R. A. Mariuzza. 2000. Luxury accommodations: the expanding role of structural plasticity in protein-protein interactions. *Structure.* 8:R137–R142.

Trautner, W. J., and M. Noyer-Weidner. 1992. High plasticity of multispecific DNA methyltransferases in the region carrying DNA target recognizing enzyme modules. *EMBO J.* 11:4445–4450.

Wilson, I. A., and L. K. Jolliffe. 1999. The structure, organization, activation and plasticity of the erythropoietin receptor *Curr. Opin. Struct. Biol.* 9:696–704.